CHEMISTRY
AN ASIAN JOURNAL

DOI: 10.1002/asia.200800317

Controlling the Structure of Manganese(II) Phosphates by the Choice and Ratio of Organophosphate and Auxiliary Ligands

Ramaswamy Murugavel,*[a, b] Subramaniam Kuppuswamy,[a] Nayanmoni Gogoi,[a] Alexander Steiner,[c] John Bacsa,[c] Ramamoorthy Boomishankar,[c] and K. G. Suresh[d]

Abstract: Tetranuclear manganese(II) phosphates $[Mn(dipp)(bpy)]_4 \cdot 4H_2O$ (**1**) and $[Mn_4(dmpp)_2(dmppH)_4(bpy)_4(H_2O)_2] \cdot H_2O$ (**2**) have been prepared from $Mn(OAc)_2 \cdot 4H_2O$ and 2,6-diisopropylphenyl phosphate ($dippH_2$) or 2,6-dimethylphenyl phosphate ($dmppH_2$) in the presence of 2,2′-bipyridine (bpy). In contrast, the reaction between $[Mn(bpy)_2(OAc)(ClO_4)] \cdot H_2O$ and $dippH_2$ affords $[Mn(bpy)_2(dippH)]_2 \cdot 2ClO_4 \cdot 2CH_3OH$ (**3**). The reactions of $Mn(OAc)_2 \cdot 4H_2O$, $dippH_2$, and pyridine (py) or 3,5-dimethylpyrazole (dmpz) in CH_3CN under reflux afford hexanuclear complexes $[Mn_6(dipp)_6(py)_8] \cdot 2CH_3CN$ (**4**) and $[Mn_6(dipp)_6(dmpz)_6(AcOH)_2] \cdot 2H_2O$ (**5**), respectively. Although compounds **1** and **2** are tetrameric, the former is a closed cubane-like structure resembling the D4R secondary building unit of zeolites, whereas the latter exists in a staircase structure with fused $Mn_2O_4P_2$ rings. The core structure of **3** contains a $Mn_2O_4P_2$ eight-membered ring that resembles the S4R building block of zeolites. Single-crystal X-ray diffraction studies reveal that compounds **4** and **5** have a similar core structure and differ from each other by the neutral ligands coordinated to manganese ions. All six phosphate ligands exist in a doubly deprotonated $[(RO)PO_3^{2-}]$ form and exhibit two types of binding modes [5.222] and [3.111]. An interesting feature of compounds **1**–**5** is that although they are oligonuclear complexes, there is an absence of oxido bridges. The magnetic properties of compounds **1**–**5** have been investigated in the temperature range 5–298 K, and it was found that all the compounds obey the Curie law.

Keywords: coordination modes · cubanes · magnetic properties · manganese · phosphorus

Introduction

The synthesis of multinuclear transition-metal cages with ligands such as PO_4^{3-} and RPO_3^{2-} has attracted interest owing to their applications in several fields, such as material chemistry and in biology.[1,2] In particular, there has been a great deal of interest in assembling polynuclear complexes of manganese with a variety of polyfunctional ligands, because of the interesting magnetic behavior of these compounds.[3] Multinuclear paramagnetic metal complexes with carboxylate ligands have been extensively studied by Christou and co-workers as well as others.[4] In recent years Winpenny and co-workers, among others, have prepared several polynuclear manganese phosphonates[5] or phosphate complexes that also incorporate carboxylate ligands.[6]

Phosphonic acids RPO_3H_2[5b,7,8] and phosphate monoesters $(RO)PO_3H_2$[9,10] are quite similar in structure and act as dianionic ligands under sufficiently basic conditions. Thus, the PO_3^{2-} ligating unit serves as a perfect platform for hosting more metal ions around each ligand. Despite their structural similarity, phosphate esters differ considerably from phosphonic acid in terms of the final products obtained after their reaction with transition-metal ions. For example, whereas alkyl or aryl phosphonic acids react with M^{II} ions to produce layered phosphonates, the introduction of an extra

[a] Prof. R. Murugavel, S. Kuppuswamy, N. Gogoi
Department of Chemistry
Indian Institute of Technology Bombay
Powai, Mumbai-400076 (India)
Fax: (+22) 2572-3480
URL: http://www.chem.iitb.ac.in/~rmv/
E-mail: rmv@chem.iitb.ac.in

[b] Prof. R. Murugavel
Centre for Research in Nanotechnology and Science
Indian Institute of Technology Bombay
Powai, Mumbai-400076 (India)

[c] Dr. A. Steiner, Dr. J. Bacsa, Dr. R. Boomishankar
Department of Chemistry, Crown Street
University of Liverpool, Liverpool, L69 7ZD (UK)

[d] Prof. K. G. Suresh
Department of Physics
Indian Institute of Technology Bombay
Powai, Mumbai-400076 (India)

oxygen atom between phosphorus and carbon (phosphate monoester) results in the isolation of discrete clusters.[9] Similarly, reactions of aluminum alkyls, alkoxides, or halides with monoaryl phosphates produce giant aluminophosphates, whereas the corresponding phosphonic acids produce smaller discrete molecules.[10] Thus, encouraged by the difference in reactivity between phosphonic acids and phosphate monoesters (similar to the differences between phosphinic acids R_2POOH and phosphate diesters $(RO)_2POOH$) and the fact that manganese phosphates have not been well investigated compared with the counterpart phosphonates, we studied the reactions of two different monoaryl esters of phosphoric acids with Mn^{II} ions in the presence of additional N-donor ligands, such as pyridine, pyrazole, and 2,2′-bipyridine with the objective to unravel different structural types of manganese phosphates. The results of this investigation are reported herein.

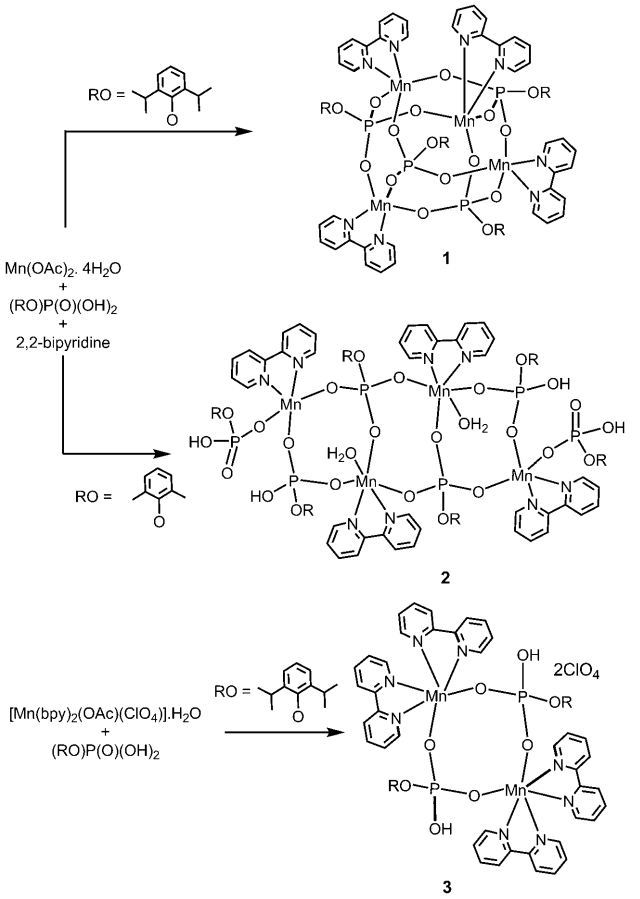

Scheme 1. Synthesis of manganese phosphates **1**–**3**.

Results and Discussion

It has been established from our recent investigations on the reactions of di-*tert*-butyl phosphate with late transition-metal ions that the use of ancillary ligands such as 2,2′-bipyridine or 1,10-phenanthroline impedes the formation of large aggregates of metal phosphates.[11] Hence, it was believed that the use of a multicenter bridging ligand such as $(RO)PO_3H_2$ along with 2,2′-bipyridine (bpy) would result in medium-sized clusters with interesting architectures.

Synthesis and Structure of $[Mn(dipp)(bpy)]_4{\cdot}4H_2O$ (1)

A methanolic solution of 2,6-diisopropylphenyl phosphate ($dippH_2$), bpy, and $Mn(OAc)_2{\cdot}4H_2O$ was stirred on a water bath and then slowly evaporated to isolate $[Mn(dipp)(bpy)]_4{\cdot}4H_2O$ (**1**) (Scheme 1). Analytically pure **1** was further characterized by IR, UV/Vis, diffuse reflectance UV/Vis, and fluorescence spectroscopy as well as single-crystal X-ray diffraction. The absence of any absorption at around $\tilde{\nu}=2350\ cm^{-1}$ indicates the absence of any precursor P–OH groups in the product, and the strong absorption observed at $\tilde{\nu}=3461\ cm^{-1}$ results from the lattice water molecules (Figure 1).

Compound **1** crystallizes in the monoclinic *I*2/*a* space group with half of the molecule in the asymmetric unit. The central core of **1** is a closed polyhedron that contains four Mn^{II} ions and four phosphorus atoms at the alternate corners of the cubane (Figure 2). Twelve oxygen atoms bridge these four Mn^{II} and four P atoms along the edges. The surface of the cubane is covered by bulky 2,6-diisopropylphenoxy groups on phosphorus and bpy on manganese ions. The arylphosphate ligands in **1** show a [3.111] bridging mode of coordination behavior as per Harris notation[12] (Table 1), and the structure is highly regular. The metric parameters of the cubic core compare well with the zinc cubanes reported by us recently.[9] The average P–O distance within the cage (1.502(3) Å) is much shorter than the formal P–O bond (1.59–1.60 Å) but significantly longer than the P=O bond (1.45–1.46 Å).[11] The average Mn–O distance (2.047(2) Å) compares well with similar Mn^{II}–O distances in other phosphonate and phosphate complexes.[5b,6,11] The average length of Mn···P edges of the cube is 3.329 Å. The average length of the face diagonal in the Mn···Mn direction is 4.724 Å, and corresponding length along the P···P distance is 4.684 Å. The length of body diagonal of the Mn_4P_4 cube is 5.758 Å. Unlike the previously reported metal phosphonate and phosphate clusters, which contain strictly tetrahedral metal atoms in the vertices, the Mn^{II} ions in **1** are five-coordinate as a result of the chelating bpy ligand on each metal. Although cubane-like structures are now fairly common in metal–phosphonate chemistry,[9] compound **1** is the first true transition-metal phosphate exhibiting this structure. Even among metal phosphonates, only main-group elements[13] such as B, Al, Ga, and In, and among transition metals Co,[5b] Cu,[8] and Zn[7] form this kind of structure. The tetrameric phosphonate $[Mn_4(\mu_3\text{-}O)(Ph_3CPO_3)_4(Py)_4]$, recently reported by Winpenny and co-workers, has a very different structure, which is best described as a trimer–monomer cage.[5b]

CHEMISTRY
AN ASIAN JOURNAL

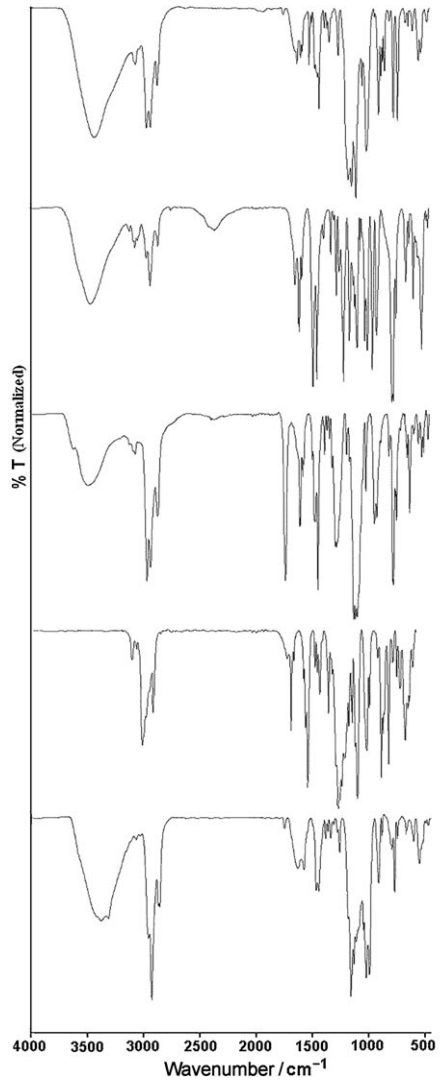

Figure 1. Infrared spectra of **1**–**5** (from top to bottom).

Synthesis and Structure of $[Mn_4(dmpp)_2(dmppH)_4(bpy)_4(OH_2)_2]\cdot H_2O$ (2)

To probe whether other structural types are possible for tetrameric (or other oligomeric) manganese phosphates, $Mn(OAc)_2\cdot 4H_2O$ was treated with less sterically substituted 2,6-dimethylphenyl phosphate ($dmppH_2$) in the presence of bpy under similar reaction conditions. A new tetranuclear complex $[Mn_4(dmpp)_2(dmppH)_4(bpy)_4(OH_2)_2]\cdot H_2O$ (**2**) was obtained as single crystals from the reaction mixture by slow evaporation of the solvent (Scheme 1). The analytically pure single crystals of **2** are insoluble in the common laboratory solvents and hence were characterized by IR, DRUV/Vis, and fluorescence spectroscopy, as well as single-crystal X-ray diffraction studies. Unlike in **1**, the presence of a broad absorption at $\tilde{\nu}=2349\,cm^{-1}$ in the IR spectrum of **2** is indicative of unneutralized P–OH groups in the cluster (Figure 1). Additional very strong broad vibrations centered at $\tilde{\nu}=3452\,cm^{-1}$ result from the coordinated and lattice water molecules. The DRUV spectrum shows three absorption maxima at $\lambda=212$, 310, and 400 nm owing to π–π^* and charge-transfer (CT) transitions, and a strong emission at $\lambda=433$ nm ($\lambda_{ex}=388$ nm). Since the free bpy or $dmppH_2$ ligand does not have any emission in this range, this fluorescence can be attributed to a CT band rather than intraligand fluorescence.[14]

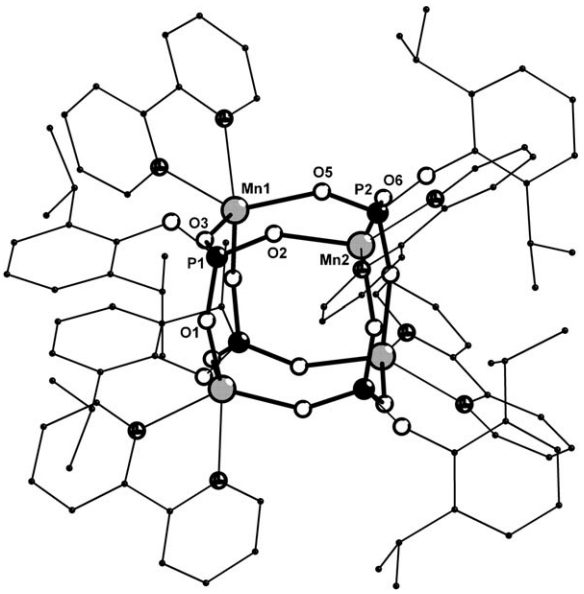

Figure 2. Molecular structure of **1** (hydrogen atoms are omitted). Selected distances [Å]: Mn–O(P) 1.992(3)–2.082(3) (av. 2.047), Mn–N 2.267(3)–2.299(3) (av. 2.286), P–O(Mn) 1.485(3)–1.513(3) (av. 1.502), P–O(Ar) 1.630(3), 1.631(3), Mn···Mn 4.72, P···P 4.68; bond angles [°]: Mn1 (*cis*) 70.6(1)–121.6(1), (*trans*) 126.5(1), 158.8(1), Mn2 (*cis*) 69.7(1)–117.1(1), (*trans*) 156.0(1), 129.3(1).

Table 1. Coordination modes of phosphate ligands in **1**–**5**.[12]

Compound	Coordination mode
1	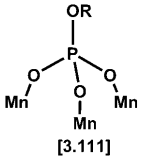 [3.111]
2	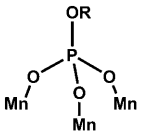 [3.111] 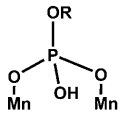 [2.110] 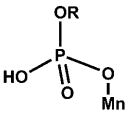 [1.100]
3	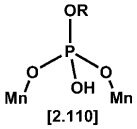 [2.110]
4 and **5**	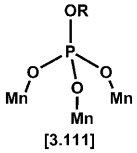 [3.111] 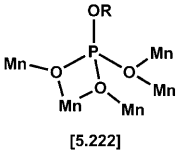 [5.222]

The crystal structure of **2** shown in Figure 3 reveals an entirely different cluster arrangement despite being a tetranuclear cluster; the Mn–O–P core in **2** has a more open ar-

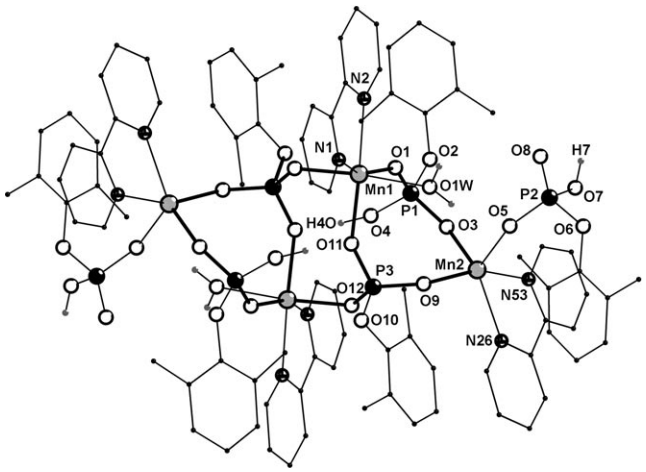

Figure 3. Molecular structure of **2** (hydrogen atoms are omitted). Selected distances [Å]: Mn–O(P) 2.046(4)–2.135(3) (av. 2.094), Mn–O(W) 2.363(4), Mn–N 2.256(4)–2.313(4) (av. 2.280), P–O(Mn) 1.489(4)–1.579(4) (av. 1.517), P–O(Ar) 1.596(4)–1.619(4) (av. 1.605), Mn1···Mn1′ 4.93, Mn1···Mn2 4.82, P1···P3 4.13, P3···P3′ 4.67; bond angles [°]: Mn1 (*cis*) 70.5(2)-105.3(1), (*trans*) 157.7(1), 161.7(1), 175.2(1), Mn2 (*cis*) 70.5(2)-100.3(2), (*trans*) 139.0(2), 159.6(2).

rangement and in fact appears to be a precursor to the cubane structure. Close inspection of the core structure reveals that the core in **2** is made up of three fused $Mn_2P_2O_4$ eight-membered ring systems in a staircase-like fashion (Figure 4). Tetranuclear manganese carboxylate cluster con-

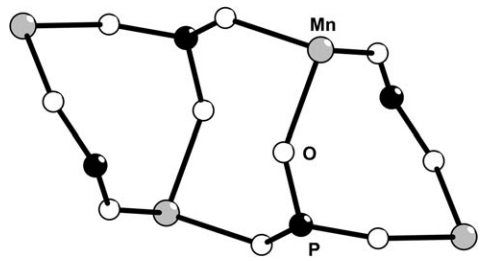

Figure 4. Staircase-like core conformation of **2**.

taining bpy ligands are fairly common, although most of these molecules have a butterfly-like Mn_4 core.[15] The staircase core found in **2** is unique among Mn_4 clusters that contain bpy ligands.

Among the three fused $Mn_2P_2O_4$ eight-membered rings, the central ring differs considerably from the two peripheral rings. The central $Mn_2P_2O_4$ ring is made up of two hexacoordinate Mn^{II} ions and two $(RO)PO_3^{2-}$ ligands. Addition of another Mn^{II} ion and a $(RO)PO_3H^-$ ligand on each side produces two more eight-membered rings, which are approximately orthogonal to the central ring in the opposite directions. To maintain the charge balance, the peripheral Mn^{II} ion is coordinated by a terminal $(RO)PO_3H^-$ ligand. Unlike the central Mn^{II} ion, the peripheral metal ions are five-coordinate and exist in a distorted trigonal bipyramidal geometry. All four metal ions in the molecule are surrounded by one bpy ligand and three phosphate oxygen atoms. The central manganese ions (Mn1) are additionally coordinated by a water molecule each and hence exist in a severely distorted octahedral geometry. The six phosphate ligands in the molecule exist in three different forms (Table 1). The phosphate ligands that are part of the central ring (P3 and P3′) are doubly deprotonated and each of them bridge three different Mn^{II} metal ions in a [3.111] fashion. The phosphate ligands that are part of the peripheral eight-membered rings (P1 and P1′) are only monodeprotonated and hence bridge only two Mn^{II} ions in a [2.110] fashion. The two terminal $(RO)PO_3H^-$ ligands (P2 and P2′) act as simple unidentate ligands through O^- termini in [1.100] fashion. The free P=O and P–OH groups of these phosphate ligands on either side of the cluster form the source of P=O···H–O–P intermolecular hydrogen bonds between the cluster as shown in Figure 5.

Synthesis and Structure of $[Mn(bpy)_2(dippH)]_2{\cdot}2ClO_4{\cdot}2CH_3OH$ (3)

After establishing the effect of substituents on the phosphate ligand in the cluster formation, we turned our attention to evaluate the role of the auxiliary bpy ligand in the cluster-formation reaction. While it is well established that the presence of one bpy ligand per metal center results in medium-sized clusters, it was anticipated that an increase in the number of bpy ligands on the metal would lead to the formation of even smaller aggregates. To test this hypothesis, we treated the precursor complex $[Mn(bpy)_2(OAc)(ClO_4)]{\cdot}H_2O$ with one equivalent of $dippH_2$ ligand under the conditions employed for the synthesis of **1** and **2**. The reaction proceeded smoothly at room temperature to produce single crystals of $[Mn(bpy)_2(dippH)]_2{\cdot}2ClO_4{\cdot}2CH_3OH$ (**3**) in very good yields (Scheme 1). The IR spectrum of **3** shows a broad absorption at $\tilde{\nu}=2356\ cm^{-1}$ arising from the presence of P–OH groups on the dippH ligand. The UV/Vis spectrum of **3** shows single absorption maxima at $\lambda=290$ nm and the fluorescence studies reveal a strong emission at $\lambda=430$ nm.

Compound **3**, which crystallizes in the triclinic $P\bar{1}$ space group, is a dicationic eight-membered ring Mn^{II} phosphate dimer (Figure 6). As expected, the presence of two bpy ligands on the metal in the precursor complex has limited the growth of the molecule by blocking four of the six maximum possible coordination sites on the metal center. Hence, the dipp ligand has also not undergone complete neutralization and exists in the form $(RO)PO_3H^-$, bridging the two metal ions in [2.110] fashion. The electroneutrality of the compound is preserved by two noncoordinating ClO_4^- ions (Table 1). The two manganese ions in the molecule are separated by 4.92 Å, which is slightly longer than the metal–metal separations in **1** (4.72 Å). The presence of free P–OH

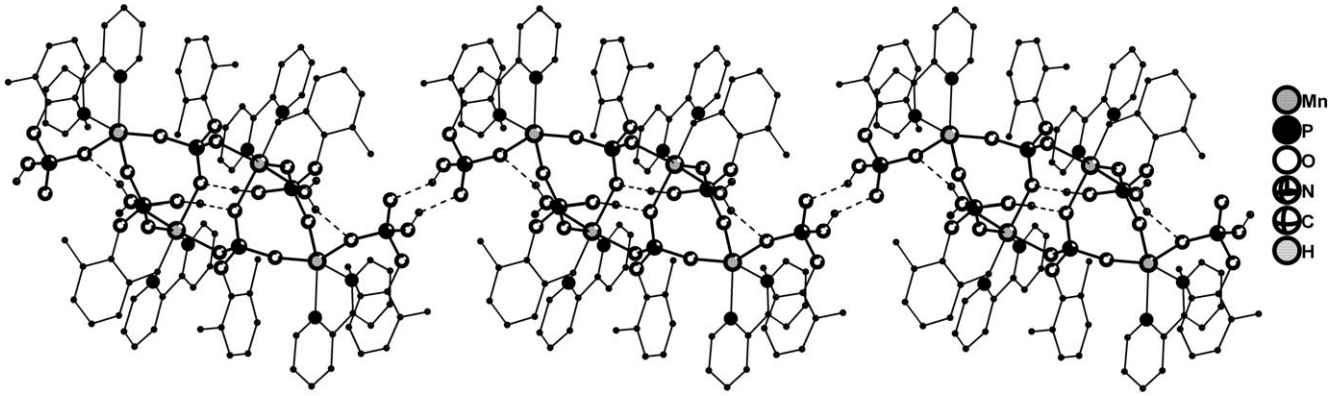

Figure 5. Intermolecular contacts of tetrameric tricyclic units of **2** through O–H···O hydrogen-bonding interactions.

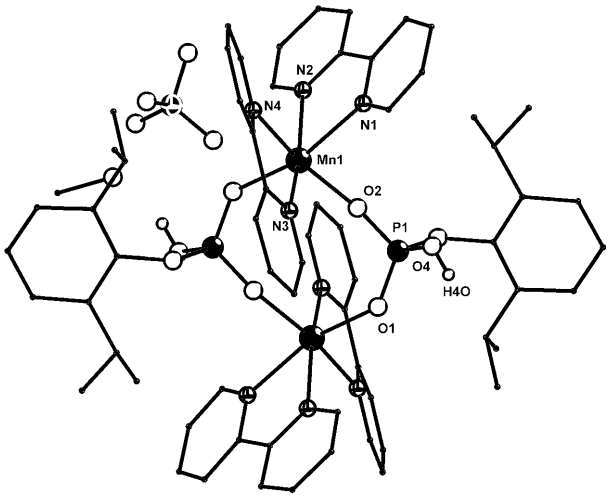

Figure 6. Cation of **3** (hydrogen atoms are omitted). Selected distances [Å]: Mn–O(P) 2.088(2), 2.091(2), Mn–N 2.270(3)–2.360(2) (av. 2.280), P–O(Mn) 1.484(2), 1.500(2), P–O(H) 1.564(2), P–O(Ar) 1.599(2), Mn1···Mn1′ 4.92, P1···P1′ 4.66; bond angles [°]: Mn1 (*cis*) 71.46(9)–98.95(9), (*trans*) 159.90(8), 162.57(8), 162.68(9).

groups, ClO_4^- anions, and bpy C–H protons leads to an interesting supramolecular aggregation, in which the molecules are arranged in a linear array with the aid of C–H···O and O–H···O hydrogen-bonding interactions (Figure 7).

Hexanuclear Manganese Phosphates $[Mn_6(dipp)_6(py)_8]\cdot 2CH_3CN$ (4) and $[Mn_6(dipp)_6(dmpz)_6(AcOH)_2]_4\cdot 2H_2O$ (5)

Whereas chelating N-donor ligands such as 2,2′-bipyridine and 1,10-phenanthroline are used to break or impede polymer formation in metal phosph(on)ate chemistry, it may be useful to use monodentate N-donor ligands, such as pyridine, as coligands to synthesize clusters larger than complexes **1**–**3**. To evaluate this possibility, we chose monodentate ligands, such as pyridine (py) and 3,5-dimethyl pyrazole (dmpz), as co-ligands. Thus, hexanuclear compounds **4** and **5** were synthesized from a three-component reaction involving $Mn(OAc)_2\cdot 4H_2O$, $dippH_2$, and py or dmpz in acetonitrile under reflux conditions (Scheme 2). Analytically pure single crystals of **4** and **5** were obtained from the reaction mixture

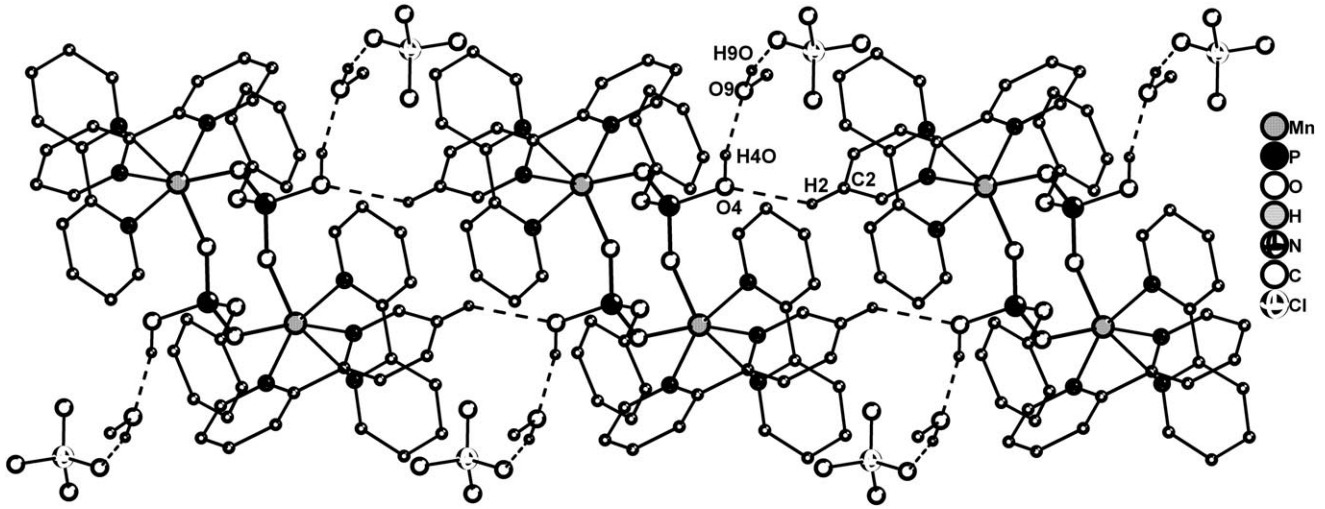

Figure 7. Hydrogen-bonded polymeric chain of **3** through C-H···O interactions. Selected hydrogen-bonding (D-H···A) distances [Å] and angles [°]: C2–H2···O4(a) 2.451, 137.43(3); O4–H40···O9(b) 1.781, 161.65(1); O9-H90···O6(b) 1.944, 163.58(3). Equivalent positions: (a) x, $+y-1$, $+z$; (b) x, y, z.

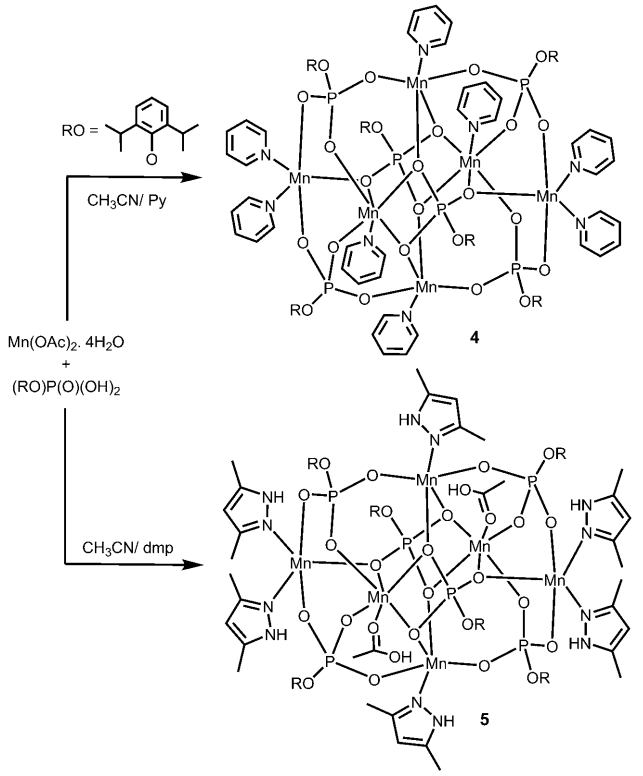

Scheme 2. Synthesis of hexameric manganese phosphates **4** and **5**.

on standing at room temperature and were characterized by elemental analysis, IR, UV/Vis, fluorescence, and EPR spectroscopic techniques, magnetic susceptibility measurements, and thermal decomposition studies.

The absence of any strong absorption at around $\tilde{\nu}=2300\ cm^{-1}$ in the IR spectra of **4** and **5** suggest that both the acidic protons of the $dippH_2$ ligand were lost during the reaction. The strong IR bands observed at around $\tilde{\nu}=1160$ and $1070\ cm^{-1}$ are readily assignable to P=O and M–O–P vibrations, respectively. Additionally, in case of **5**, the N–H and solvent water O–H stretching frequencies appear as a broad vibration at $\tilde{\nu}=3452\ cm^{-1}$, and the carbonyl C=O stretching band of the coordinated acetic acid appears at $\tilde{\nu}=1601\ cm^{-1}$. The absorption and emission properties of **4** and **5** differ significantly in solution and the solid state. In solution, **4** and **5** show a single absorption maximum at around $\lambda=270$ ($\varepsilon=305\ L\,mol^{-1}\,cm^{-1}$) and 340 nm ($\varepsilon=270\ L\,mol^{-1}\,cm^{-1}$), respectively, in DMSO and emit at longer wavelength ($\lambda=415$ nm) as a narrow emission ($\lambda_{ex}=345$ nm). Unlike in solution, the solid-state diffuse-reflectance UV/Vis spectrum of **4** exhibits three absorption maxima at $\lambda=214$, 265, and 315 nm (221, 270, and 302 for **5**). Despite having multiple absorptions, compounds **4** and **5** show a sharp single emission band in the solid state at around $\lambda=425$ nm ($\lambda_{ex}=380$ nm).

Molecular Structure of $[Mn_6(dipp)_6(py)_8]\cdot 2\,CH_3CN$ (4)

The single-crystal X-ray structural analysis of compound **4** shows that it is a centrosymmetric hexanuclear cluster (Figure 8). As described above, hexanuclear clusters are uncommon among manganese phosphates/phosphonates and only a very few structural motifs involving six Mn ions have been reported.[5,6] The molecular structure **4** represents a new structural motif for manganese phosphate/phosphonates. The three-dimensional cluster **4** resembles a rugby ball and is composed of six Mn^{II} ions, six multidentate $(RO)PO_3^{2-}$ phosphate anions, and eight monodentate neutral pyridine molecules. An interesting aspect of the structure of **4** is the absence of oxido ligands in the molecule, although many polynuclear metal phosphonate complexes are built around either μ-oxido or μ-hydroxido ligands.[2,3] The central manganese ions Mn1, Mn1′, Mn2, and Mn2′ form the core of the complex, and are held together by two phosphate ligands. This core embraces two more Mn^{II} ions and four more phosphate ligands to produce the hexameric clus-

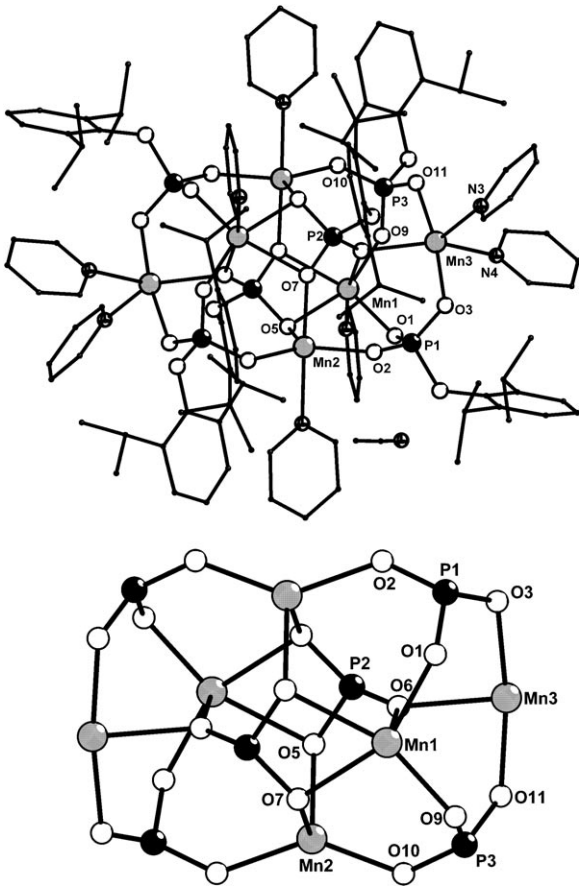

Figure 8. Molecular structure of **4** (lattice CH_3CN molecules and hydrogen atoms are omitted for clarity). Selected bond lengths [Å]: Mn–O(P) 2.048(3)–2.330(3) (av. 2.161), Mn–N 2.229(4)–2.318(4) (av. 2.263), P–O(Mn) 1.500(3)–1.531(3) (av. 1.514), P–O(Ar) 1.603(3)–1.630(3) (av. 1.621); cluster dimensions [Å]: O12···O12′ 11.65, P3···P3′ 8.47, Mn3···Mn3′ 8.45, Mn2···Mn2′ 5.42, Mn1···Mn1′ 5.26, Mn1···Mn2 3.78, P2···P2′ 3.66.

ter. Pyridine co-ligands used in the reaction fill up the coordinative unsaturation on all the six metal centers and thus impede any further cluster growth.

The six Mn^{II} ions exist in three different coordination environments with two different coordination geometries. The central Mn1 ions (Mn1 and Mn1′) are hexacoordinate in a distorted octahedral geometry; they are surrounded by five phosphate oxygen atoms and one pyridine molecule (MO_5N). The Mn2 and Mn3 ions that lie on the periphery of the cluster are five-coordinate and exist in distorted trigonal-bipyramidal geometry. While Mn2 and Mn2′ ions are surrounded by four phosphate oxygen atoms and one pyridine ligand, the Mn3 and Mn3′ centers are coordinated by three phosphate oxygen atoms and two pyridine ligands. The phosphate ligands in the molecule show two different types of ligation behavior. Whereas the two central phosphate ligands (P2 and P2′) are hexadentate (bidentate through each of three oxygen atom) and bridge five of the total six manganese ions (Figure 9), the other four phosphate ligands are tridentate and symmetrically bridge three different metal ions as shown in Figure 8 (bottom). Thus, according to Harris notations these ligands exhibit [5.222] and [3.111] modes of coordination, respectively (Table 1).[12]

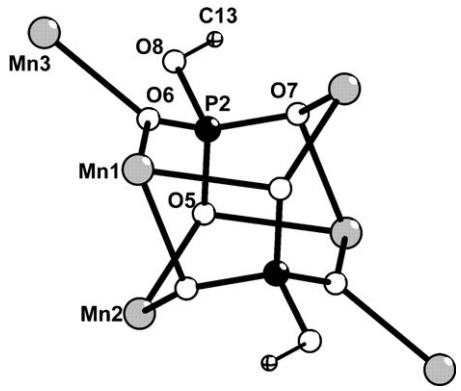

Figure 9. Core of **4** showing the two hexadentate phosphate ligands with [5.222] coordination mode holding the six manganese ions together.

The average Mn–O(P) and Mn–N bond lengths are comparable (2.161 and 2.263 Å) to those found in compounds **1**–**3**. As expected, the average P–O(Mn) distance (1.514 Å) is significantly shorter than the P–O(Ar) distance (1.621 Å). The twelve *cis* angles in the coordination sphere of octahedral Mn1 vary over a wide range (63.39(9)–111.0(1)°), whereas the three *trans* angles deviate considerably from linearity (151.0(1), 157.3(1), 171.4(1)°). The other two types of manganese ions (Mn2 and Mn3) also exhibit large deviations from the expected angles for an ideal trigonal-bipyramidal geometry. For example, the *cis* angles around Mn2 vary in the range 88.4(1)–93.6(1)°, while the corresponding angles around Mn3 are in the range 82.8(1)–95.2(1)°. The angles in the trigonal plane around Mn2 and Mn3 are 109.1(1), 113.5(1), and 137.2(1)° (Mn2) and 90.8(2), 125.1(1), and 144.2(1)° (Mn3), respectively, indicating much larger distortions around Mn3. The *trans* angles around Mn2 and Mn3 are 174.5(1) and 170.8(1)°, respectively. The size of the inorganic core excluding the organic substituents on the cluster is 11.7 Å. The Mn3···Mn3′ distance is 8.45 Å and the corresponding P3···P3′ distance is 8.47 Å. The central tetranuclear star-shaped unit exhibit both short and large Mn···Mn′ distances (Mn1···Mn1′ = 5.26 Å, Mn2···Mn2′ 5.42 Å and Mn1···Mn2 3.78 Å).

Molecular Structure of $[Mn_6(dipp)_6(dmpz)_6(AcOH)_2]_4 \cdot 2H_2O$ (5)

X-ray quality single crystals of $[Mn_6(dipp)_6(dmpz)_6(AcOH)_2]_4 \cdot 2H_2O$ (**5**) were obtained by the recrystallization of crude product from CH_3CN. Compound **5** crystallizes in the centrosymmetric monoclinic space group $P2_1/n$ with half of the molecule in the asymmetric unit. A view of the refined structure of **5** is shown in Figure 10 along with selected structural parameters. The overall molecular architecture of

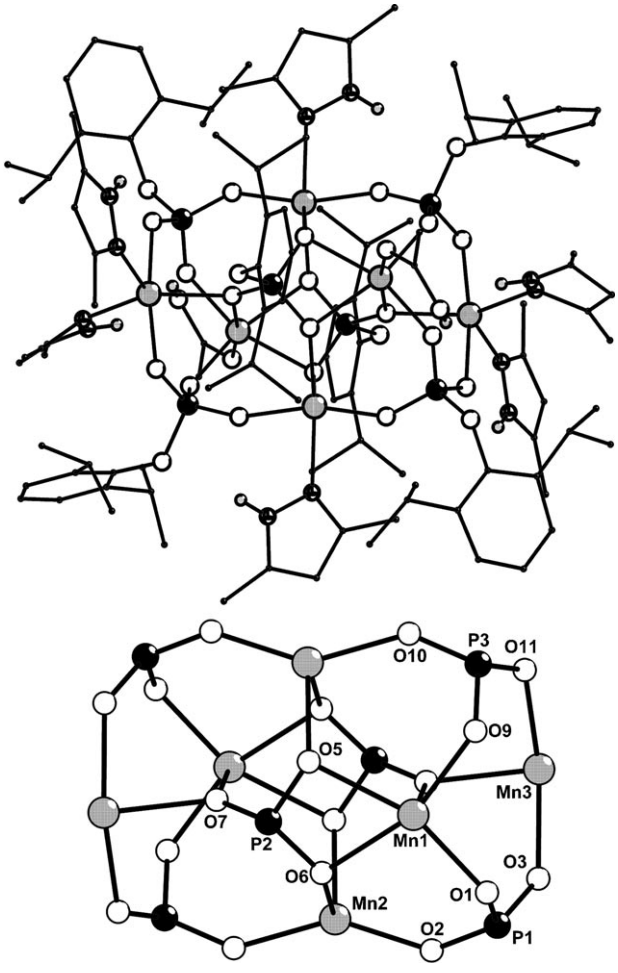

Figure 10. Molecular structure of **5** (lattice H_2O molecules and hydrogen atoms are omitted for clarity). Selected bond lengths [Å]: Mn–O(P) 2.030(3)–2.299(3) (av. 2.159), Mn–N 2.149(5)–2.258(5) (av. 2.210), P–O(Mn) 1.498(4)–1.533(3) (av. 1.512), P–O(Ar) 1.589(3)–1.630(4) (av. 1.614); cluster dimensions [Å]: O3···O3′ 11.69, P1···P1′ 8.62, Mn3···Mn3′ 8.59, Mn2···Mn2′ 5.50, Mn1···Mn1′ 5.10, Mn1···Mn2 3.67, P2···P2′ 3.69.

5 is very similar to that of **4**. The major difference between the structures of **4** and **5** is in the monodentate ligand coordinated to the central Mn1 ions. The coordination environment around both Mn2 and Mn3 ions is invariant in both the structures.

The dmpz ligand in **5** plays the role of pyridine in **4**. However, there are only six dmpz ligands in the structure of **5** and these are coordinated to the Mn2, Mn2′, Mn3, and Mn3′ centers. The sixth coordination site on Mn1 in **5** is surprisingly taken up by acetic acid, which is a by-product in the reaction. The presence of this ligand in the OAc^- form (rather than AcOH form) can be ruled out both in terms of the color of the compound (colorless; presence of a Mn^{II}/Mn^{III} system would have resulted in a dark-colored product) and the C–O and M–O–(C) distances observed for **5**. Further, the acidic proton on the AcOH was also located from the difference map and refined to good convergence both for its position and isotropic thermal parameters. Further, the temperature-dependent magnetic behavior of **5** is similar to **4** (see below). Hence, it can be concluded that compound **5**, as in the case of **4**, is a Mn_6^{II} complex and not a $Mn_2^{III}Mn_4^{II}$ system. The coordination geometry and the associated bond lengths and angles around the Mn ions in **5** are also similar to those found for **4**. The Mn1 ion is octahedral with significant deviations from ideal angles (*cis* angles 64.5(1)–101.8(1)°; *trans* angles 157.1(1)–170.5(1)°). Similarly, both trigonal-bipyramidal Mn2 and Mn3 ions are also considerably distorted. The *cis* angles for Mn2 and Mn3 lie in the ranges 83.4(2)–103.9(1)° and 84.1(1)–108.0(2)°, respectively. The trigonal angles around both Mn2 and Mn3, however, add up to approximately 360° (Mn2: 104.7(1), 112.2(1), 143.1(2)°; Mn3: 105.4(3), 120.8(2), 132.5(2)°). The size of the inorganic core excluding the organic substituents on the cluster is 11.69 Å. The Mn3···Mn3′ distance across the cluster is 8.59 Å and the corresponding P1···P1′ separation is 8.62 Å. The central tetranuclear star-shaped unit Mn···Mn′ distances are Mn1···Mn1′ = 5.10 Å, Mn2···Mn2′ 5.50 Å, and Mn1···Mn2 3.67 Å. The P2···P2′ distance is 3.69 Å.

Thermal Decomposition Studies

Thermal decomposition of compounds **1–5** was observed by both thermogravimetric analysis (TGA) and bulk thermolysis. The products obtained by bulk thermolysis were subsequently characterized by powder X-ray diffraction (PXRD) measurements. Whereas the products obtained by the thermal degradation of **1** and **3** yield a complicated PXRD pattern, compound **2** decomposes cleanly to produce a mixture of MnP_2O_7 and $Mn(PO_3)_2$. Thermal decomposition of the hexanuclear compounds **4** and **5** leads exclusively to the pyrophosphate MnP_2O_7.

Magnetic Studies

The temperature-dependent magnetic moments of all the five complexes were measured to evaluate any metal–metal interactions in these systems. Magnetic susceptibility measurements were carried out for all five samples in a dc field over a temperature range of 5–300 K by using a vibrating sample magnetometer. All samples are paramagnetic over the entire temperature range investigated. All were found to obey the Curie law very well. The effective (paramagnetic) moment was calculated by fitting to the Curie law. The dinuclear derivative **3** showed a paramagnetic moment of 4.9 μ_B (per Mn^{2+} ion) at room temperature, which is quite close to the expected spin-only moment for Mn^{2+} of 5.9 μ_B. The tetranuclear and hexanuclear manganese phosphates, however, showed a considerable decrease in the magnetic moments at room temperature. This decrease is much more marked for the hexanuclear derivatives **4** and **5** (2.2 and 2.1 μ_B) than for the tetranuclear complexes **1** and **2** (3.2 and 3.0 μ_B).

On the basis of the spectroscopic and optical studies described above and the measured magnetic moments, mixed valency in the cluster compounds can be ruled out. Therefore, it is clear that in all the compounds, there is a decrease from the theoretical moment value. The high moment observed in **3** is consistent with the fact that in this case antiferromagnetic exchange interactions are mediated by two μ_2-phsophate bridges only. However, in all other compounds, the large decrease in moment could be ascribed to the stronger antiferromagnetic interactions mediated through phosphate ligands exhibiting larger denticities.

Conclusions

In conclusion, we have shown that it is possible to produce medium-sized metal phosphate clusters by the introduction of either a chelating auxiliary ligand, such as 2,2′-bipyridine, or monodentate N-donor ligands, such as pyridine or pyrazole. The synthesis of **1** and **2**, the two different tetrameric structures obtained from two different phosphate esters, showcases the effect of organic substituents on phosphoric acid in determining which kind of structure is formed for the given nuclearity of the cluster. The synthesis of **1** and **2** (tetramers) versus **4** and **5** (hexamers) points to the fact that monodentate terminal ligands are poorer blockers of oligo- and polymerization than the bidentate chelating ligands. Compound **1** represents the first example of the incorporation of a five-coordinate metal center in a D4R cubane cluster not only for metal phosphates but also for metal phosphonates and siloxanes.[16] Similarly, the molecular structure of **2** represents a staircase cluster, which could be conceived as a possible intermediate in the formation of the cubane cluster **1** through folding of the fused eight-membered rings (Scheme 3). The synthesis of **2** further demonstrates that by placing an additional bpy ligand on the metal center, the nuclearity of the complex can be further reduced to a simple dimer. An additional outcome of the results reported herein relates to the denticity of the phosphate ligand. As the nuclearity of the complex increases, the denticity of the phosphate ligands also increases among the five complexes reported (Table 1). Whereas the monoarylphosphate ligand exhibits a [2.110] mode of coordination in dinuclear complex

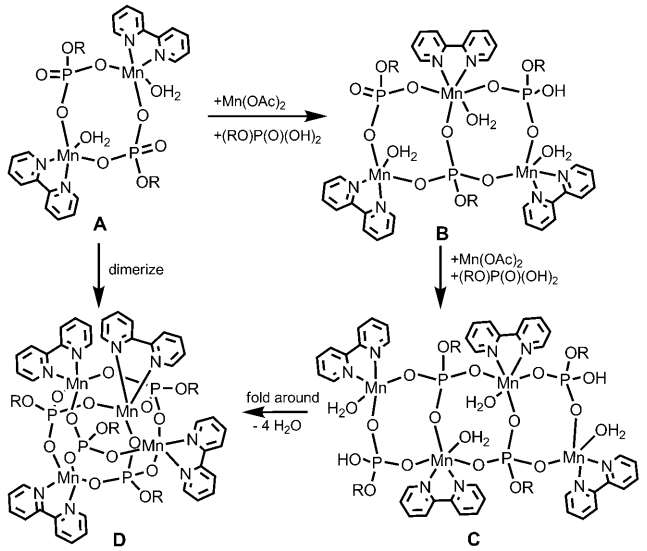

Scheme 3. Plausible pathway for cubane formation.

3, it exhibits a [3.111] mode of coordination in the tetranuclear complexes **1** and **2** (in addition to being [2.110] and [1.100] in the case of **2**). The denticity increases sharply for the hexameric clusters **4** and **5**, [5.222] and [3.111]. The [5.222] mode of binding is the first chelating mode of coordination observed in transition-metal phosphate chemistry (even for first-row transition-metal phosphonates, the chelating mode of coordination is unknown).

The diversity of the structures described herein clearly indicates that the isolation of further structural types of manganese phosphates is possible by variation of the oxidation state of manganese ion, the auxiliary ligands, and attendant changes on the structure of phosphate substituents. We are currently exploring these aspects with the aim to prepare larger clusters with interesting magnetic behavior.

Experimental Section

Methods and Materials

All starting materials and products were found to be stable towards moisture and air, and hence no specific precautions were taken to exclude air during the manipulation of the compounds. Infrared spectra were obtained on a Perkin–Elmer Spectrum One FTIR spectrometer as KBr diluted discs. The melting points were measured in glass capillaries and were reported uncorrected. Microanalyses were performed on a Thermo Finnigan (FLASH EA 1112) microanalyzer. Thermogravimetric analysis was carried out on a Perkin–Elmer Pyris thermal analysis system under a stream of nitrogen gas at a heating rate of 10 K per minute. X-ray powder diffraction data were collected on a Philips X'Pert Pro X-ray diffraction system by using monochromated $Cu_{K\alpha_1}$ radiation ($\lambda = 1.5406$ Å). UV/Vis spectra were obtained on Shimdzu UV-260 spectrophotometer and the fluorescence was recorded on Perkin–Elmer LS-55 luminescence spectrometer. Variable-temperature magnetic susceptibility measurements were performed on a Quantum Design PPMS-vibrating-sample magnetometer. EPR measurements were carried out on a Varian model 109C E-line X-band spectrometer fitted with a quartz dewar for measurements at 77 K (liquid nitrogen) and the spectra were calibrated using tetracyanoethylene.

Commercial-grade solvents were purified by employing conventional procedures and were freshly distilled prior to their use.[17] Commercially available starting materials such as pyridine (S.d.Fine-Chem.), 2,2′-bipyridine (S.d.Fine-Chem.), and $Mn(OAc)_2{\cdot}4H_2O$ (E.Merck) were used as received. 3,5-Dimethylpyrazole,[17] 2,6-diisopropylphenyl phosphate,[18] 2,6-dimethylphenyl phosphate,[18] and $[Mn(bpy)_2(OAc)(ClO_4)]{\cdot}H_2O$[19] were synthesized as described previously. ***Caution! Perchloric acid and its salts are potentially explosive and should be handled with care.***

*Synthesis and Characterization Data of $[Mn(dipp)(bpy)]_4{\cdot}4H_2O$ (**1**)*

Solid $Mn(OAc)_2{\cdot}4H_2O$ (245 mg, 1 mmol) was dissolved in methanol (30 mL), and solid bpy (156 mg, 1 mmol) and $dippH_2$ (258 mg, 1 mmol) were added. The reaction mixture was heated on a water bath for 30 min and filtered. Yellow single crystals of **1** were obtained from the filtrate after 2–3 days at 25 °C. M.p.: >275 °C; Yield: 0.4 g (83 %); elemental analysis: calcd (%) for $C_{88}H_{108}Mn_4N_8O_{20}P_4$ ($M_r = 1941.51$): C 54.44, H 5.61, N 5.77; found: C 54.65, H 5.39, N 5.60; IR (KBr, cm^{-1}): $\tilde{\nu}$ = 3412(br), 3098(w), 3069(w), 3027(w), 2963(s), 2923(m), 2866(m), 1595(s), 1576(m), 1490(w), 1472(m), 1439(vs), 1381(w), 1360(w), 1337(w), 1316(w), 1256(m), 1164(vs), 1057(m), 1014(vs), 995(s), 903(s), 878(m), 804(w), 766 cm^{-1} (vs); UV/Vis (CH_3OH, nm): $\lambda_{max} = 295$ ($\varepsilon = 825$ $L\,mol^{-1}\,cm^{-1}$); fluorescence ($\lambda_{ex} = 338$ nm, CH_3OH): 428 nm. $\phi = 0.0004$; DRUV/Vis: $\lambda_{max} = 212$, 312, and 425 nm; fluorescence ($\lambda_{ex} = 381$ nm, Solid state): 426 nm; EPR: $g = 2.00$ (298 K), 1.98 (77 K).

*Synthesis and Characterization Data of $[Mn_4(dmpp)_2(dmppH)_4(bpy)_4(OH_2)_2]{\cdot}H_2O$ (**2**)*

Solid $Mn(OAc)_2{\cdot}4H_2O$ (245 mg, 1 mmol) was dissolved in methanol (30 mL) and solid bpy (158 mg, 1 mmol) and $dmppH_2$ (303 mg, 1.5 mmol) were added sequentially. The reaction mixture was heated on a water bath for 30 min and filtered. Yellow single crystals of **2** were obtained from the filtrate after 3–4 days at 25 °C. M.p: >275 °C; Yield: 0.44 g (84 %, based on $dmppH_2$); elemental analysis: calcd (%) for for $C_{88}H_{96}Mn_4N_8O_{27}P_6$ ($M_r = 2103.36$): C 50.25, H 4.60, N 5.32; found: C 50.60, H 4.36, N 5.33; IR (KBr, cm^{-1}): $\tilde{\nu}$ = 3452(br), 3107(w), 3057(w), 2956(w), 2922(m), 2854(w), 2349(br), 1634(m), 1601(s), 1594(s), 1575(w), 1474(vs), 1440(vs), 1381(w), 1317(w), 1266(m), 1244(w0, 1203(vs), 1152(s), 1105(w), 1083(s), 1056(w), 992(s), 948(vs), 908(s), 759 cm^{-1} (vs); DRUV/Vis: $\lambda_{max} = 212$, 311, and 400 nm; fluorescence ($\lambda_{ex} = 381$ nm, Solid state): $\lambda_{max} = 433$ nm; TGA: temp. range °C (% weight loss): 105–170 (2.5, $-3H_2O$), 170–500 (59.8, loss of all organic groups), 500–600 (2.6, $-5H_2O$); EPR: $g = 2.01$ (298 K), 1.99 (77 K).

*Synthesis and Characterization Data of $[Mn(bpy)_2(dippH)]_2{\cdot}2ClO_4{\cdot}2CH_3OH$ (**3**)*

A solution of $dippH_2$ (258 mg, 1 mmol) in methanol (10 mL) was added to a solution (MeOH, 20 mL) of $[Mn(bpy)_2(OAc)(ClO_4)]{\cdot}H_2O$ (543 mg, 1 mmol). The resultant solution was stirred until the solution became almost clear. The reaction mixture was then filtered and the filtrate was kept on a bench top for crystallization at 25 °C. Yellow single crystals of **3** were obtained from the reaction mixture after 24 h. M.p: 215–216 °C; Yield: 0.6 g (80 %, based on $dippH_2$); elemental analysis: calcd (%) for $C_{66}H_{76}Cl_2Mn_2N_8O_{18}P_2$ ($M_r = 1512.1$): C 52.43, H 5.07, N 7.41; found: C 52.14, H 4.96, N 7.51; IR (KBr, cm^{-1}): $\tilde{\nu}$ = 3461(br), 3063(w), 2961(s), 2926(m), 2866(m), 2356(br), 1601(s), 1595(s), 1575(m), 1566(m), 1490(w), 1473(s), 1439(vs), 1380(w), 1359(w), 1336(w), 1317(m), 1245(s), 1184(s), 1159(m), 1119(vs), 1105(s), 1090(vs), 1013(s), 939(s), 916(m), 808(w), 766(s), 740(m), 645(m), 624 cm^{-1} (s); UV/Vis (CH_3OH, nm): $\lambda_{max} = 290$ ($\varepsilon = 1641$ $L\,mol^{-1}\,cm^{-1}$); fluorescence ($\lambda_{ex} = 351$ nm, CH_3OH): $\lambda_{max} =$ 430 nm. $\phi = 0.0003$; DRUV/Vis: $\lambda_{max} = 215$, 305, and 392 nm; fluorescence ($\lambda_{ex} = 383$ nm, solid state): $\lambda_{max} = 429$ nm; EPR: $g = 1.99$ (298 K), 1.98 (77 K).

*Synthesis and Characterization Data of $[Mn_6(dipp)_6(py)_8]{\cdot}2CH_3CN$ (**4**)*

Solid $Mn(OAc)_2{\cdot}4H_2O$ (245 mg, 1 mmol) and $dippH_2$ (258 mg, 1 mmol) were dissolved in CH_3CN (30 mL) under reflux conditions for 3 h. The reaction mixture was subsequently filtered and pyridine (1 mL) was added. The resultant mixture was kept for crystallization at 25 °C. Color-

less crystals of **4** were obtained from the reaction mixture after 2–3 days. M.p: >275 °C; Yield: 0.4 g (96%, based on $dippH_2$); elemental analysis: calcd (%) for evacuated sample $[Mn_6(dipp)_6(py)_8]$ ($C_{112}H_{142}N_8O_{24}P_6Mn_6$; M_r = 2499.87): C 53.81, H, 5.73, N 4.48; found: C 54.37, H 5.13, N 4.66; IR (KBr, cm^{-1}): $\tilde{\nu}$ = 3065(w), 2964(s), 2867(m), 1601(s), 1487(w), 1467(m), 1445(vs), 1379(w), 1359(w), 1336(m), 1256(m), 1164(vs), 1130(vs), 1102(s), 1069(s), 1037(s), 988(vs), 900(s), 878(m), 801(w), 768 cm^{-1} (s); UV/Vis (DMSO, nm): λ_{max} = 270 (ε = 305 $L mol^{-1} cm^{-1}$); fluorescence (λ_{ex} = 348 nm, DMSO): λ_{max} = 412 nm. ϕ = 0.0023; DRUV/Vis: λ_{max} = 214, 265, and 315 nm; fluorescence (λ_{ex} = 382 nm, solid state): λ_{max} = 425 nm; EPR: g = 2.00 (298 K), 2.00 (77 K).

*Synthesis and Characterization Data of $[Mn_6(dipp)_6(dmpz)_6(AcOH)_2]_4 \cdot 2H_2O$ (**5**)*

Solid $Mn(OAc)_2.4H_2O$ (245 mg, 1 mmol) and $dippH_2$ (258 mg, 1 mmol) were dissolved in CH_3CN (30 mL) and 3,5-dimethyl pyrazole (96 mg, 1 mmol) was added. The reaction mixture was heated under reflux for 3 h, filtered, and the filtrate was allowed to crystallize. Colorless crystals of **5** were obtained from the reaction mixture after 2–3 days at 25 °C. M.p: >275 °C; Yield: 0.35 g (81%); elemental analysis: calcd (%) for $C_{106}H_{160}N_{12}O_{30}P_6Mn_6$ (M_r = 2598.0): C 49.01, H 6.21, N 6.47; found: C 49.28, H 6.40, N 6.89; IR (KBr, cm^{-1}): $\tilde{\nu}$ = 3452(br), 3107(w), 3057(w), 2956(w), 2922(m), 2854(w), 1634(m), 1601(s), 1594(s), 1575(w), 1474(vs), 1440(vs), 1381(w), 1317(w), 1266(m), 1244(w0, 1203(vs), 1152(s), 1105(w), 1083(s), 1056(w), 992(s), 948(vs), 908(s), 759 cm^{-1} (vs); UV/Vis (DMSO, nm): λ_{max} = 340 (ε = 270 $L mol^{-1} cm^{-1}$); fluorescence (λ_{ex} = 344 nm, DMSO): λ_{max} = 416 nm. ϕ = 0.0035; DRUV/Vis: λ_{max} = 221, 270, and 302 nm; fluorescence (λ_{ex} = 381 nm, solid state): λ_{max} = 430 nm; EPR: g = 2.01 (298 K), 2.00 (77 K).

Single-Crystal X-ray Diffraction Studies

Intensity data for **1**–**3** were collected on a Bruker Smart Apex diffractometer and data for **4** and **5** were measured on an Oxford Xcalibur CCD diffractometer. All calculations were carried out with the programs in WinGX module. The structure was solved by direct methods in most cases by using SIR-92.[20] The final refinement of the structure was carried out using full least-squares methods on F^2 with SHELXL-97.[21] Selected crystal data are given in Table 2. CCDC-698822 (**1**), 698823 (**2**), 698824 (**3**), 698825 (**4**), and 698826 (**5**), contains the supplementary crystallographic data for this paper. These data can be obtained free of charge from The Cambridge Crystallographic Data Centre at www.ccdc.cam.ac.uk/data_request/cif.

Acknowledgements

This work was supported by DST, New Delhi. We thank the DST funded National Single Crystal Diffraction Facility at IIT-Bombay for the diffraction data and SAIF, IIT-Bombay for the spectral data. NG thanks CSIR, New Delhi for a research fellowship.

[1] a) M. G. Walawalkar, H. W. Roesky, R. Murugavel, *Acc. Chem. Res.* **1999**, *32*, 117–126; b) R. Murugavel, M. G. Walawalkar, M. Dan, H. W. Roesky, C. N. R. Rao, *Acc. Chem. Res.* **2004**, *37*, 763–774; c) R. Murugavel, M. G. Walawalkar, R. Pothiraja, C. N. R. Rao, A. Choudhury, *Chem. Rev.* **2008**, *108*, 3549–3655.

[2] a) A. Clearfield, *Curr. Opin. Solid State Mater. Sci.* **1996**, *1*, 268–278; b) G. Alberti, *Comprehensive Supramolecular Chemistry Vol. 7* (Ed.: J. M. Lehn), Pergamon, Oxford, U.K., **1996**; c) G. Cao, H. G. Hong, T. E. Mallouk, *Acc. Chem. Res.* **1992**, *25*, 420–427; d) M. B. Dines, P. M. DiGiacomo, *Inorg. Chem.* **1981**, *20*, 92–97; e) D. M. Poojary, B. Zhang, A. Clearfield, *Angew. Chem.* **1994**, *106*, 2420–2422; *Angew. Chem. Int. Ed. Engl.* **1994**, *33*, 2324–2326; f) A. Clearfield, U. Costantino, *Solid State Supramolecular Chemistry and Layered Solids Vol. 7* (Eds.: G. Alberti, T. Bein), Pergamon, New York, **1996**, p. 107; g) M. E. Thompson, *Chem. Mater.* **1994**, *6*, 1168–1175; h) Y. Zhang, A. Clearfield, *Inorg. Chem.* **1992**, *31*, 2821–2826; i) G. Cao, V. M. Lynch, L. N. Yacullo, *Chem. Mater.* **1993**, *5*, 1000–1006, and references therein.

[3] a) R. Sessoli, D. Gatteschi, A. Caneschi, M. A. Novak, *Nature* **1993**, *365*, 141–143; b) R. Sessoli, H.-L. Tsai, A. R. Schake, S. Wang, J. B. Vincent, K. Folting, D. Gatteschi, G. Christou, D. N. Hendrickson, *J. Am. Chem. Soc.* **1993**, *115*, 1804–1816; c) Z. Y. Du, A. V. Prosvirin, J. G. Mao, *Inorg. Chem.* **2007**, *46*, 9884–9894.

[4] a) O. M. Yaghi, M. O'Keeffe, N. Ockwig, H. K. Chae, M. Eddaoudi, J. Kim, *Nature* **2003**, *423*, 705–714; b) M. Soler, W. Wernsdorfer, K.

Table 2. Crystal data and structure refinement for **1**–**5**.

Compound	**1**	**2**	**3**	**4**	**5**
Identification code	SK224	SK725	SK357	Newrm222	Newrm225
Formula	$C_{88}H_{108}Mn_4N_8O_{20}P_4$	$C_{88}H_{98}Mn_4N_8O_{27}P_6$	$C_{66}H_{76}Cl_2Mn_2N_8O_{18}P_2$	$C_{116}H_{148}Mn_6N_{10}O_{24}P_6$	$C_{106}H_{166}Mn_6N_{12}O_{32}P_6$
Fw	1941.46	2105.32	1512.07	2581.90	2635.97
T [K]	213(2)	205(2)	213(2)	150(2)	150(2)
Crystal system	monoclinic	monoclinic	triclinic	monoclinic	monoclinic
Space group	$I2/a$	$P2_1/c$	$P\bar{1}$	$P2_1/c$	$P2_1/n$
a [Å]	23.904(3)	16.777(3)	12.0664(18)	15.2767(3)	16.479(1)
b [Å]	15.272(2)	10.961(2)	12.082(2)	26.5857(5)	20.451(1)
c [Å]	26.655(5)	27.447(9)	13.568(2)	16.1998(4)	19.433(1)
α [°]	90	90	76.73(2)	90	90
β [°]	104.217(18)	108.89(3)	77.117(19)	109.502(3)	91.634(70
γ [°]	90	90	70.770(18)	90	90
V [Å^3]	9433(2)	4776(2)	1794.2(5)	6202.0(2)	6202.0(2)
Z	4	2	1	2	2
D(calcd) [g cm^{-3}]	1.367	1.464	1.399	1.383	1.337
μ [mm^{-1}]	0.662	0.697	0.544	0.741	0.708
crystal size [mm^3]	0.5×0.4×0.2	0.50×0.30×0.26	0.2×0.2×0.2	0.32×0.28×0.22	0.32×0.28×0.22
θ range [°]	2.05 to 24.24	2.02 to 24.14	1.81 to 24.30	2.93 to 25.00	3.12 to 25.00
no. of reflections collected	29612	25867	11449	31564	34855
no. of observed reflections ($I_0 > 2\sigma(I_0)$)	7276	7417	5266	10836	11506
GOF	0.879	0.788	0.997	1.041	0.950
$R1(I_0 > 2\sigma(I_0))$	0.0449	0.0464	0.0396	0.0541	0.0720
$wR2$ (all data)	0.1190	0.0853	0.1065	0.1461	0.1903
largest hole and peak [e·Å^{-3}]	−0.483, 0.521	−0.306, 0.471	−0.403, 0.660	−1.300, 0.417	−0.678, 0.603

Folting, M. Pink, G. Christou, *J. Am. Chem. Soc.* **2004**, *126*, 2156–2165; c) V. M. Mereacre, A. M. Ako, R. Clérac, W. Wernsdorfer, G. Filoti, J. Bartolomé, C. E. Anson, A. K. Powell, *J. Am. Chem. Soc.* **2007**, *129*, 9248–9249.

[5] a) S. Konar, A. Clearfield, *Inorg. Chem.* **2008**, *47*, 3489–3491; b) M. Wang, C. Ma, D. Yuan, M. Hu, C. Chen, Q. Liu, *New J. Chem.* **2007**, *31*, 2103–2110; c) V. Baskar, M. Shanmugam, E. C. Sanudo, M. Shanmugam, D. Collison, E. J. L. Mclnnes, Q. Wei, R. E. P. Winpenny, *Chem. Commun.* **2007**, 37–39; d) Y.-S. Ma, Y. Song, Y.-Z. Li, L.-M. Zheng, *Inorg. Chem.* **2007**, *46*, 5459; e) Y.-S. Ma, H.-C. Yao, W.-J. Hua, S.-H. Li, Y.-Z. Li, L.-M. Zheng, *Inorg. Chim. Acta* **2007**, *360*, 1645; f) M. Shanmugam, G. Chastanet, T. Mallah, R. Sessoli, S. J. Teat, G. A. Timco, R. E. P. Winpenny, *Chem. Eur. J.* **2006**, *12*, 8777–8785; g) M. Shanmugam, M. Shanmugam, G. Chastanet, R. Sessoli, T. Mallah, W. Wernsdorfer, R. E. P. Winpenny, *J. Mater. Chem.* **2006**, *16*, 2576–2578; h) H.-C. Yao, Y.-Z. Li, Y. Song, Y.-S. Ma, L.-M. Zheng, X.-Q. Xin, *Inorg. Chem.* **2006**, *45*, 59–65; i) S. Maheswaran, G. Chastanet, S. J. Teat, T. Mallah, R. Sessoli, W. Wernsdorfer, R. E. P. Winpenny, *Angew. Chem.* **2005**, *117*, 5172–5176; *Angew. Chem. Int. Ed.* **2005**, *44*, 5044–5048; j) E. K. Brechin, R. A. Coxall, A. Parkin, S. Parsons, P. A. Tasker, R. E. P. Winpenny, *Angew. Chem.* **2001**, *113*, 2772–2775; *Angew. Chem. Int. Ed.* **2001**, *40*, 2700–2703.

[6] G.-Q. Bian, T. Kuroda-Sowa, H. Konaka, M. Hatano, M. Maekawa, M. Munakata, H. Miyasaka, M. Yamashita, *Inorg. Chem.* **2004**, *43*, 4790–4792.

[7] a) R. Murugavel, S. Shanmugan, *Chem. Commun.* **2007**, 1257–1259; b) R. Murugavel, S. Shanmugan, *Dalton Trans.* **2008**, 5358–5367.

[8] V. Chandrasekhar, L. Nagarajan, R. Clérac, S. Ghosh, S. Verma, *Inorg. Chem.* **2008**, *47*, 1067–1073.

[9] a) R. Murugavel, S. Kuppuswamy, R. Boomishankar, A. Steiner, *Angew. Chem.* **2006**, *118*, 5662–5666; *Angew. Chem. Int. Ed.* **2006**, *45*, 5536–5540; b) R. Murugavel, S. Kuppuswamy, S. Randoll, *Inorg. Chem.* **2008**, *47*, 6028–6039; c) R. Murugavel, S. Kuppuswamy, *Inorg. Chem.* **2008**, *47*, 7686–7694; d) R. Murugavel, S. Shanmugan, *Organometallics* **2008**, *27*, 2784–2788; e) R. Murugavel, S. Shanmugan, S. Kuppuswamy, *Eur. J. Inorg. Chem.* **2008**, 1508–1517. .

[10] a) R. Murugavel, S. Kuppuswamy, *Angew. Chem.* **2006**, *118*, 7180–7184; *Angew. Chem. Int. Ed.* **2006**, *45*, 7022–7026; b) R. Murugavel, S. Kuppuswamy, *Chem. Eur. J.* **2008**, *14*, 3869–3873.

[11] a) R. Pothiraja, M. Sathiyendiran, R. J. Butcher, R. Murugavel, *Inorg. Chem.* **2005**, *44*, 6314–6323; b) R. Pothiraja, M. Sathiyendiran, R. J. Butcher, R. Murugavel, *Inorg. Chem.* **2004**, *43*, 7585–7587; c) R. Murugavel, M. Sathiyendiran, R. Pothiraja, R. J. Butcher, *Chem. Commun.* **2003**, 2546–2547; d) M. Sathiyendiran, R. Murugavel, *Inorg. Chem.* **2002**, *41*, 6404–6411; e) R. Murugavel, M. Sathiyendiran, *Chem. Lett.* **2001**, 84–85; f) R. Murugavel, M. Sathiyendiran, M. G. Walawalkar, *Inorg. Chem.* **2001**, *40*, 427–434.

[12] Harris notation describes the binding mode as [*X.Y1Y2Y3..Yn*], where *X* is the overall number of metal atoms bound by the whole ligand and each value of *Y* refers to the number of metal atoms attached to the different donor atoms. See: R. A. Coxall, S. G. Harris, D. K. Henderson, S. Parsons, P. A. Tasker, R. E. P. Winpenny, *J. Chem. Soc. Dalton Trans.* **2000**, 2349–2356.

[13] a) M. G. Walawalkar, R. Murugavel, H. W. Roesky, H.-G. Schmidt, *Inorg. Chem.* **1997**, *36*, 4202–4207; b) M. G. Walawalkar, S. Horchler, S. Dietrich, D. Chakraborty, H. W. Roesky, M. Schäfer, H.-G. Schimdt, G. M. Sheldrick, R. Murugavel, *Organometallics* **1998**, *17*, 2865–2868; c) J. Pinkas, D. Chakraborty, Y. Yang, R. Murugavel, M. Noltemeyer, H. W. Roesky, *Organometallics* **1999**, *18*, 523–528.

[14] Y.-F. Zhou, R.-H. Wang, B.-L. Wu, R. Cao, M.-C. Hong, *J. Mol. Struct.* **2004**, *697*, 73–79.

[15] a) E. Libby, J. K. McCusker, E. A. Schmitt, K. Folting, D. N. Hendrickson, G. Christou, *Inorg. Chem.* **1991**, *30*, 3486–3495; b) E. Bouwman, M. A. Bolcar, E. Libby, J. C. Huffman, K. Folting, G. Christou, *Inorg. Chem.* **1992**, *31*, 5185–5192; c) B. Albela, M. S. El. Fallah, J. Ribas, K. Folting, G. Christou, D. N. Hendrickson, *Inorg. Chem.* **2001**, *40*, 1037–1044; d) G. Aromí, S. Bhaduri, P. Artus, J. C. Huffman, D. N. Hendrickson, G. Christou, *Polyhedron* **2002**, *21*, 1779–1786.

[16] R. Murugavel, A. Voigt, M. G. Walawalkar, H. W. Roesky, *Chem. Rev.* **1996**, *96*, 2205–2236.

[17] Vogel's *Text Book of Practical Organic Chemistry*, 5th ed., Langman Group, Essex, Harlow, UK, **1989**.

[18] G. M. Kosolapoff, C. K. Arpke, R. W. Lamb, H. Reich, *J. Chem. Soc. C* **1968**, 815–818.

[19] B.-H. Ye, X.-M. Chen, F. Xue, L. N. Ji, T. C. W. Mak, *Inorg. Chim. Acta* **2000**, *299*, 1–8.

[20] A. Altomare, G. Cascarano, C. Giacovazzo, A. Gualardi, *J. Appl. Crystallogr.* **1993**, *26*, 343–350.

[21] G. M. Sheldrick, SHELXL-97, Program for Structure Refinement, University of Göttingen: Germany, **1997**.

Received: August 16, 2008
Published online: November 28, 2008

